Al 3*p* valence and excitonic states in $GaSb/Al_{0.3}Ga_{0.7}Sb$ and $GaAs/Al_{0.3}Ga_{0.7}As$ heterostructures as a function of growth process

P. Jonnard, F. Vergand, and C. Bonnelle
Laboratoire de Chimie Physique Matière et Rayonnement, URA 176, Université Pierre et Marie Curie, 11 rue Pierre et Marie Curie, 75231 Paris Cedex 05, France

M. Leroux and J. Massies
Centre de Recherches sur l'Hétéro-épitaxie et ses Applications, CNRS-Sophia Antipolis, 06560 Valbonne, France
(Received 30 September 1996; revised manuscript received 17 January 1997)

Density of states (DOS) in $GaSb/Al_{0.3}Ga_{0.7}Sb$ systems are studied by electron-induced x-ray emission spectroscopy (EXES) and compared to previous results we have obtained for $GaAs/Al_{0.3}Ga_{0.7}As$ systems. The Al 3*p* valence DOS are analyzed in the bulk ternary compounds, in heterostructures, and in interfacial zones 30 Å thick, this thickness being equivalent to that of heterostructure layers. Large changes of the Al 3*p* valence DOS are seen, depending on the preparation conditions of the samples whose quality was checked by photoluminescence. For heterostructures having a small interface roughness, localization of states on the whole valence band of barriers is evidenced. This localization is attributed to bidimensional effects that largely dominate the interface effects. In contrast, for heterostructures having interfaces of lower quality, interface interaction and localization are competitive. Core excitonic transitions seen by EXES confirm that localization of Al states in the barriers exists for superlattices with abrupt interfaces. [S0163-1829(97)03223-2]

I. INTRODUCTION

During the last two decades, the III-V semiconductor compounds have been extensively studied from the point of view of both basic physics and applications. The physical studies are specifically concerned with the electronic and optical properties. The band structure of bulk binary compounds has been calculated.[1–6] Their density of valence states (valence DOS) has been studied by photoemission[7–10] and x-ray emission.[5,11,12]

Heterostructures based on III-V compounds, such as quantum wells and superlattices, are of continuously growing technical and scientific interest. In these systems, the composition modulation along the growth axis induces a change of the periodicity that modifies the electronic structure and the mixing of the valence states. In the plane of layers, the carrier motion is free. Perpendicular to them, one expects that the carriers are delocalized for samples having short periods due to tunneling through the lateral potential barriers, whereas they are confined in potential minima for larger periodicities. This results in the appearance of two-dimensional (2D) subbands in the electronic structure.

Any real heterostructure can contain imperfections such as interface roughness, point defects, dislocations, impurities, etc. Due to the small thicknesses along the growth axis, one expects that interface effects can modify the band structure. These effects vary according to the quality of interfaces, thus the growth conditions, and these play an important role on the valence DOS characteristics.

Consequently the valence DOS of heterostructures can be affected by a possible simultaneous confinement in the layer planes and the presence of eventual perturbations at interfaces. It is the purpose of the present paper to investigate the relative importance of the perturbations due to the bidimensionality and to the interface-related defects on the valence DOS of III-V heterostructures. For this, the spectral valence DOS are analyzed in interfacial zone between bulk binary and ternary compounds and by integrating the information on several periods of the heterostructures.

Electron-induced x-ray emission spectrometry (EXES) allows the analysis of spectral valence DOS in a bulk material, a multilayer, and an interfacial zone buried under some hundreds of angströms.[12] From this experimental method, we studied the Al 3*p* DOS in the $Al_{0.3}Ga_{0.7}As$ ternary compound, at the $GaAs/Al_{0.3}Ga_{0.7}As$ interface, in a GaAs (30 Å)/$Al_{0.3}Ga_{0.7}As$ (31 Å) superlattice and in a single quantum well GaAs (30 Å) between two barriers $Al_{0.3}Ga_{0.7}As$ (31 Å).[13] In fact, only Al, the element present in one type of layer (here the barriers) gives information on characteristics of either the interface or the whole sample.

In this paper, we analyze by EXES the Al 3*p* valence DOS of $GaSb/Al_{0.3}Ga_{0.7}Sb$ systems prepared with and without growth interruption at the binary/ternary interfaces, growth interruptions being well known to improve the interface smoothness.[14–16] We compare the Al 3*p* valence DOS in the barriers to those obtained at the interface and also to previous results obtained for the $GaAs/Al_{0.3}Ga_{0.7}As$ systems, which are briefly recalled. We show that the interface effect is completely dominated by the bidimensionality effect in the case where growth interruptions are performed. Core excitonic emissions are also observed. In parallel, photoluminescence spectroscopy has been performed with the aim of evidencing the importance of growth interruptions on the well states near the forbidden energy gap.

After a brief description of the sample characteristics and the experimental method, we present the EXES and photoluminescence spectra and we discuss the respective role of the interfaces and of the bidimensionality on the DOS as a function of superlattice interface abruptness.

TABLE I. Deposition conditions of the GaAs/$Al_{0.3}Ga_{0.7}As$ and GaSb/$Al_{0.3}Ga_{0.7}Sb$ systems during the molecular beam epitaxy. For each sample, the energy E_0 of incident electrons used to obtain Al $K\beta$ spectra is indicated. In the case of bulk samples, the second energy is that used to obtain the interface spectra.

Sample label	T substrate (°C)	Deposition rates (μm/h)		Growth interruption	Electron energy (eV)
		Ga(As,Sb)	AlGa(As,Sb)		
$B1$	540	0.82	1.16	Yes	4500 and 2100
SL1	540	0.82	1.16	No	4500
SL2	540	0.82	1.16	Yes	4500
$B2$	600	0.35	0.5	Yes	4300 and 2050
SL3	600	0.35	0.5	Yes	5000
QW1	600	0.35	0.5	Yes	3500

II. EXPERIMENT

A. Sample preparation

All the samples were grown on (100) GaSb Te-doped substrates, by molecular beam epitaxy. Reflection high-energy electron diffraction (RHEED) oscillation patterns were used to control the growth process.[17] They were protected with a 100-Å-thick GaSb ultimate layer. The sample, labeled $B1$, is $Al_{0.3}Ga_{0.7}Sb$ bulk 800 Å thick (Table I). The two samples, labeled SL1 and SL2, are superlattices consisting of 100 periods of $Al_{0.3}Ga_{0.7}Sb$ (30.5 Å)/GaSb (30.5 Å), each period being 10 monolayers (ML) $Al_{0.3}Ga_{0.7}Sb$/10 ML GaSb. The deposition rates were 0,82 and 0,34 μm/h for GaSb and AlSb, respectively, and the substrate temperature was 540 °C. For SL1, the growth was made continuously. In contrast, for SL2, the growth was interrupted 5 s after each layer under vapor pressure of antimony (Sb_4).

In Table I, characteristics of the $Al_{0.3}Ga_{0.7}As$ systems are also recalled. The sample, labeled $B2$, is $Al_{0.3}Ga_{0.7}As$ bulk 1500 Å thick. The sample SL3 is a superlattice consisting of 24 periods of $Al_{0.3}Ga_{0.7}As$ (31 Å)/AlAs (30 Å). That labeled QW1 is a 30-Å-thick single quantum well surrounded by two 31-Å-thick $Al_{0.3}Ga_{0.7}As$ barriers. The growth was interrupted after each layer under As_4 pressure.

B. Analysis method

EXES is especially useful in the study of electronic properties of interfaces. In this method, ionization of an nlj core subshell is produced in an atom of atomic number Z by interaction with an incident electron. The created core hole state can relax by radiative transition involving a valence electron.[18] The energy distribution of the emitted photons (spectral distribution) describes the distribution of a hole in the valence DOS (here in Al $3p$ states) broadened by the energy distribution of the initial state and multiplied by the transition probability. This probability can be assimilated to a constant along the emission band and, within this approximation, changes of the spectral DOS reveal changes of valence DOS. Local (given Z) and partial (given symmetry $s,p,d,\ldots$) DOS are obtained. The local character is due to the localization of the core hole involved in the transition and the partial character to the dipole selection rules. In contrast, by photoemission one obtains the total valence DOS weighted by the photoabsorption cross sections, which vary according to the symmetry of states along the valence band.

The analyzed depth is that where incident electrons have an energy higher than the ionization threshold $E_{nlj}(Z)$ of the element Z under study. In the case of a material A covered by a film of another material, we set the energy of incident electrons so that a chosen thickness of the material A is analyzed by taking into account the electron energy loss through the overlayer and in the material A. With the incident energy of the electrons, E_0, close to the threshold, the method is convenient to obtain spectral valence DOS and characterize the bonds in very thin layers. By progressively increasing E_0, buried interfaces as well as multilayers can be analyzed.[19] In contrast, photoemission analyzes only superficial layers.

X-ray spectra were obtained by means of a Johann-type spectrometer with a bent $(10\bar{1}0)$ quartz crystal (500 mm radius) monochromator.[20] The incident electron beam made a 10° angle with respect to the normal of the sample. The current density is a few mA/cm^2. The temperature of the water-cooled sample is between 30 and 60 °C. The detector is a gas flow counter (90% Ar, 10% CH_4). The spectral resolution is about 2×10^{-4} and the photon energy is determined to within 0.2 eV. The Al $K\beta(3p\text{-}1s)$ emission was analyzed. The Al $1s$ ionization threshold is $\approx$1560 eV. The energy distribution associated to an Al $1s$ hole is a Lorentz curve about 0.4 eV wide. The instrumental function of the spectrometer can be fitted by a Lorentz curve about 0.2 eV wide.[20] The general shape of the Al $3p$ DOS is little modified by the convolution with the Lorentz distribution $\mathcal{L}$, taking into account the broadening due to the lifetime of the states and to the instrumental function.

The values of incident energies E_0 are reported in Table I. For the superlattices, E_0 was chosen so that the major part of the sample is analyzed. For sample QW1, E_0 was 3500 eV in order to obtain an appreciable value of the ionization cross section. For GaSb(As)/$Al_{0.3}Ga_{0.7}Sb$(As) interfaces of samples $B1$ and $B2$, E_0 was chosen from excitation curves (number of photons at the maximum of the emission measured versus E_0) so that (i) the analyzed thickness is of the same order as the thickness of the layers of the superlattices and (ii) an appreciable number of photons is counted in order to obtain correct statistics. For each value of E_0 we calculate the ratio $r(x)=I(x)/I(\infty)$, where $I(x)$ is the intensity coming from a thickness x of the sample and $I(\infty)$ the intensity coming from infinite thickness. The calculation is made by means of a semi-empirical model that takes into account the energy and angular distributions of incident and backscat-

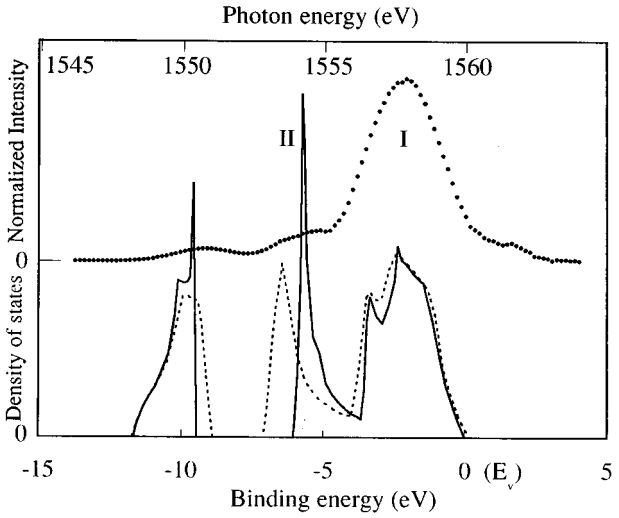

FIG. 1. Comparison of the Al 3p spectral DOS for bulk $Al_{0.3}Ga_{0.7}Sb$ (dots) with the total DOS calculated for AlSb (solid line) from Ref. 3 and GaSb (dashed line) from Ref. 6.

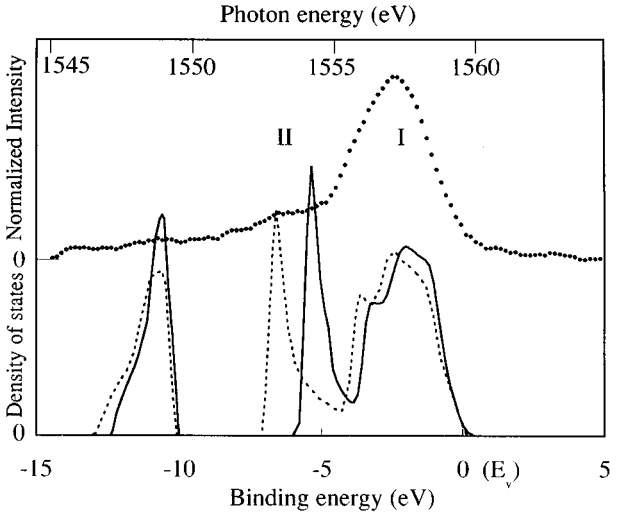

FIG. 2. Comparison of the Al 3p spectral DOS for bulk $Al_{0.3}Ga_{0.7}As$ (dots) with the total DOS calculated for AlAs (solid line) from Ref. 2 and GaAs (dashed line) from Ref. 6.

tered electrons, electroionization cross sections, and absorption of the emitted photons.[21,22] The electroionization cross section strongly decreases as the electron energy comes close to the threshold. The number of incident electrons that can interact also strongly decreases. So we consider that the relevant analyzed thickness is the one giving $r(x)=0.80$. For $B1$ and $B2$, the thicknesses of the interfacial zone, x, are 30 and 40 Å, respectively.

No emission line of Ga, As, and Sb is present in the Al $3p$-$1s$ emission range. The quasilinear background due to the bremsstrahlung is subtracted and the spectra are normalized to their maximum. The curves are smoothed by using the locally weighted least-squares error method. Statistical fluctuations are lower with the bulk and superlattice (3% at the top) than with the interface (20% at the top). The curves represent the normalized intensities versus the photon energy. The energy scale referred to the top of the valence band E_v is also indicated.

Photoluminescence spectra were recorded at various temperatures using a closed-cycle He cryostat. The 4880-Å line of an Ar laser was used (≈ 100 W/cm^2) and luminescence was detected using an N_2-cooled Ge detector.

III. RESULTS

A. EXES analysis

The Al 3p spectral DOS in bulk $Al_{0.3}Ga_{0.7}Sb$ is presented in Fig. 1 and compared to the total DOS calculated for AlSb (Ref. 3) and GaSb (Ref. 6). The curves are adjusted relative to the top of the valence band E_v. This point is determined by fitting the valence-band edge by a linear law $(E-E_v)$ convoluted with a Lorentzian curve $\mathcal{L}$ of full width at half maximum (FWHM) $L_{1/2}$ equal to 0.6 eV.

Calculations of the total DOS have been made for III-V ternary compounds with the aim of determining the band offset in heterojunctions.[23] In these calculations valence DOS have been investigated between the top of the band and about 3–4 eV below but not on the whole band width, making the comparison with our data difficult. The DOS of III-V ternary compounds are assumed to be close to those of binary compounds, shift and broadening being expected, depending on the nature of the cations. This justifies that we compare our results to the total DOS calculated for binary compounds. The AlSb DOS is calculated by empirical pseudo-potential method[3] and the GaSb DOS by the self-consistent linear muffin-tin orbital (LMTO) method.[6] The shapes of both DOS are similar: a strongly structured peak, 3–4 eV wide, located at the same energy in both compounds, is present near the top of the valence band. It corresponds to strongly mixed Al 3p, or Ga 4p and Sb 5p states. A narrow peak appears in the energy range near -5 eV; this peak corresponds essentially to Al 3s, or Ga 4s, and some Sb 5p states. It is shifted towards the higher binding energies when the atomic number of the trivalent element increases. The peak situated near -10 eV is mainly due to Sb 5s states; it is at the same energy for the two compounds and is separated from other states by the ionic gap.

The main peak of the Al 3p spectral DOS, labeled I in Fig. 1, is in coincidence with doubly peaked maximum of the calculated DOS attributed to the Al 3p states. Towards the higher and lower binding energies the experimental peak presents unresolved structures that correspond to the structures of the calculated DOS. In the energy range labeled II, a weak feature is seen in the spectral DOS at an energy intermediate between that of the peak II calculated for AlSb and GaSb. We attribute it to Al 3p states mixed with Al 3s states. In the energy range of Sb 5s states, the Al 3p spectral DOS is not zero; this shows that a slight mixing exists between the Al 3p and Sb 5s states.

By analogy, we show in Fig. 2 the Al 3p spectral DOS of bulk $Al_{0.3}Ga_{0.7}As$ (Ref. 13) compared to the total DOS recently calculated for GaAs by the self-consistent LMTO method[6] and to the AlAs total DOS calculated by the self-consistent linearized augmented plane wave method.[2] Comparison of Figs. 1 and 2 shows that the DOS of $Al_{0.3}Ga_{0.7}Sb$ and $Al_{0.3}Ga_{0.7}As$ are similar.

In Fig. 3 we compare the Al 3p spectral DOS obtained for both superlattices SL1 and SL2 to that observed for bulk

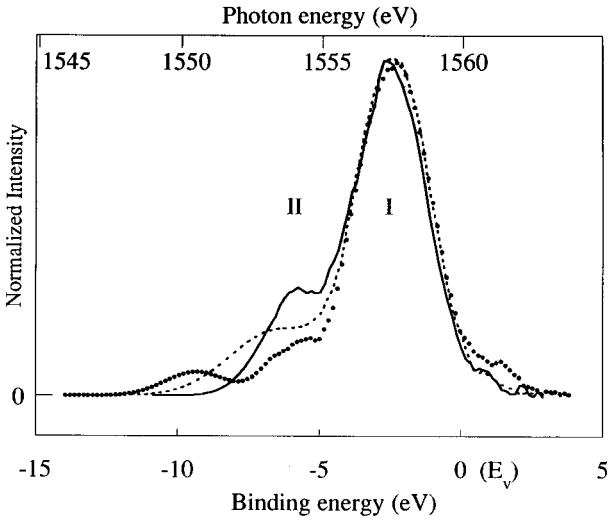

FIG. 3. Comparison of the Al $3p$ spectral DOS for bulk $Al_{0.3}Ga_{0.7}Sb$ (dots) and for $GaSb/Al_{0.3}Ga_{0.7}Sb$ superlattices SL1 (dashed line) and SL2 (solid line).

$Al_{0.3}Ga_{0.7}Sb$. The main change in the SL2 spectral DOS is the observation of a pronounced peak (labeled peak II) in the range where the Al $3p$ are mixed with the Al $3s$ states. The main peak is narrower and shifted towards the higher binding energies and the structure below the ionic gap disappears. For SL1 the spectral DOS does not show the pronounced peak II but increases weakly and spreads in the ionic gap. The main peak is similar to that of the bulk ternary compound.

The narrow and pronounced feature that has been seen in the energy range II for the superlattice SL3 is of same type as that observed for SL2 but of weaker intensity (Fig. 4). For the barriers that surround the single quantum well the feature is more pronounced than for SL3 and a narrowing of the main peak is observed.

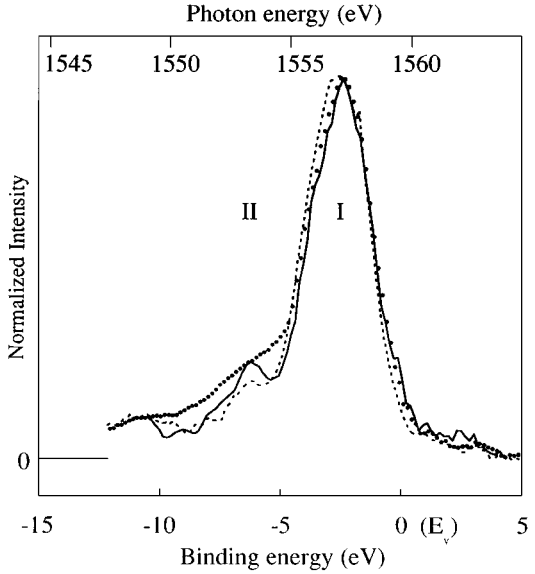

FIG. 4. Comparison of the Al $3p$ spectral DOS for bulk $Al_{0.3}Ga_{0.7}As$ (dots), for the $GaSb/Al_{0.3}Ga_{0.7}As$ superlattice SL3 (dashed line) and for the single quantum well surrounded by two barriers (solid line).

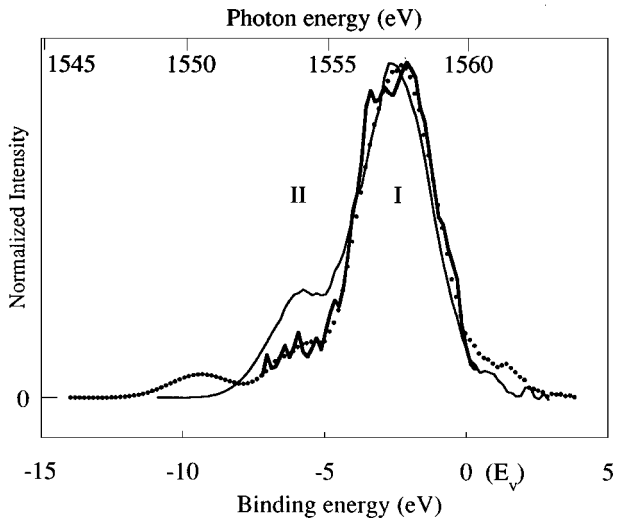

FIG. 5. Comparison of the Al $3p$ spectral DOS for bulk $Al_{0.3}Ga_{0.7}Sb$ (dots), for the $GaSb/Al_{0.3}Ga_{0.7}Sb$ superlattice SL2 (thin solid line) and for the $GaSb/Al_{0.3}Ga_{0.7}Sb$ interface (thick solid line).

With the aim of determining the spectral characteristics of the interface between GaSb and $Al_{0.3}Ga_{0.7}Sb$, we have analyzed the Al $3p$ DOS in the $GaSb/Al_{0.3}Ga_{0.7}Sb$ interfacial region of sample $B1$ (30 Å thick). This curve is compared in Fig. 5 to the bulk and SL2 spectral DOS. For the interface, no increase of the spectral DOS is seen at the position of the peak II. A 0.3–0.4-eV broadening of the main peak is observed at the top of the valence band. It must be noted that the intensity is weak for the interface because the number of atoms that contribute to the spectrum is small. The spectral DOS is reproduced only in the range where appreciable intensity is present.

Faint structures are observed above E_v in bulk and superlattice spectra. They correspond to transitions from excited states located in the band gap or mixed with conduction states. The energy and the relative intensity of these structures have been obtained by decomposing the spectral curves in the region 1558–1563 eV [Figs. 6(a)–6(c)]. The valence-band edge is fitted as previously indicated. The structures are fitted by convoluting a Lorentzian curve of FWHM $L_{1/2}$ with a Gaussian curve of FWHM $G_{1/2}$. The Lorentzian curve is the same as that used for the valence-band edge. The Gaussian curve accounts for the statistical distribution of the excited states created in the material. All the parameters are listed in Table II.

B. Photoluminescence analysis

A direct way of evidencing the importance of growth interruptions on superlattice interface abruptness is to look at optical properties near the forbidden energy gap.

The photoluminescence (PL) spectra of samples SL1 and SL2 at low temperature are presented in Fig. 7. They spread $\approx$30 meV, with a main peak accompanied by high- and low-energy shoulders. The energies and shapes of the two spectra are different. The PL maximum of SL1 is at 987 meV, significantly higher than that of SL2 located at 978 meV. It is the same for the high-energy shoulders, located at 1001 meV in SL1 and 996 meV in SL2. On the other hand,

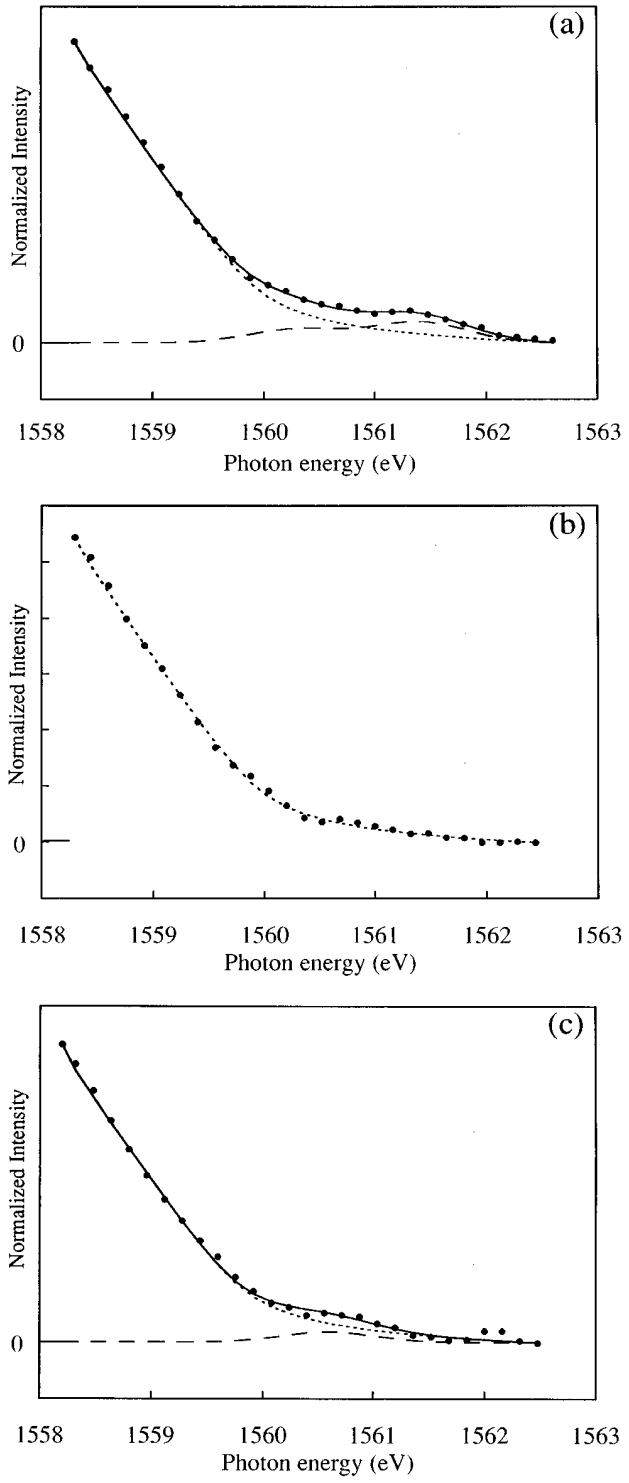

FIG. 6. Decomposition of the Al 3p spectral DOS in the regions of the valence-band edge and the optical gap for bulk $Al_{0.3}Ga_{0.7}Sb$ (a) and for superlattices $GaSb/Al_{0.3}Ga_{0.7}Sb$ SL1 (b) and SL2 (c) Dots: experiment; short-dashed line: valence edge; long-dashed line: structures in the optical gap; full line: sum of the valence-band edge and structures.

the low-energy shoulder is at 973 meV in SL1, i.e., only 28 meV lower in energy than the 1001-meV band, whereas it is at 945 meV, i.e., at much lower energy in SL2.

In Fig. 8 is reported the dependence with excitation intensity and temperature of the PL spectra of SL1. At 9 K, the

TABLE II. Parameters of the decomposition of the valence-band edge and the optical gap of the $GaSb/Al_{0.3}Ga_{0.7}Sb$ systems. $L_{1/2}$ is the full width at half maximum (FWHM) of the Lorentzian, which takes into account the lifetime and instrumental broadenings, E_v is the position of the top of the valence band (± 0.2 eV), E_{struct} is the position of the structure(s) in the optical gap (± 0.1 eV), and $G_{1/2}$ is the FWHM of the Gaussian (± 0.1 eV), which accounts for the statistical distribution of the excited states.

Sample label	$L_{1/2}$ (eV)	E_v (eV)	Energy of structure (eV)	$G_{1/2}$ (eV)
$B1$	0.6	1559.9	1561.4 1560.3	0.5 0.5
SL1	0.6	1559.9		
SL2	0.6	1559.9	1560.6	0.55

decrease of the excitation power leads to the disappearance of the high- and low-energy shoulders (lower two spectra in Fig. 8). This suggests that the main peak at 987 meV is the superlattice ground state. The increase of the sample temperature results in a progressive quenching of this main peak in favor of the high- and low-energy shoulders (1001 and 973 meV), which dominate the spectrum at ≈ 40 K. This suggests first that a thermal transfer of carriers occurs from the ground state towards a large density of states level located higher in the conduction band and second that the 973-meV band is related to this level.

Similar experiments for SL2 show that in the same temperature range, the PL spectra are dominated by the main peak at 978 meV and the low-energy shoulder. Intensity is totally quenched at 40 K. Having in mind that the difference between the main peak and the high-energy shoulder is larger in SL2 than in SL1 (18 meV instead of 14 meV), it appears that the thermal transfer is less efficient in SL2 than in SL1. This is in accordance with the fact that at 9 K the intensity of the high-energy shoulder is higher in SL1 than in SL2, as Fig. 7 shows.

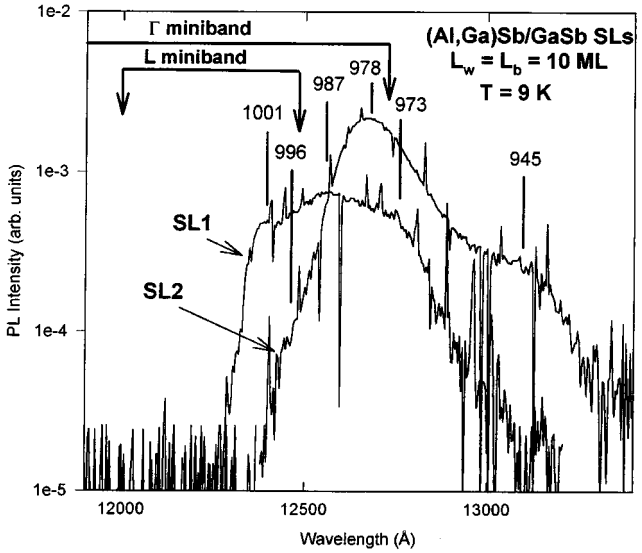

FIG. 7. Photoluminescence spectra at 9 K of $GaSb/Al_{0.3}Ga_{0.7}Sb$ superlattices SL1 and SL2. The arrows indicate the calculated miniband limits of a 10 ML/10 ML $GaSb/Al_{0.30}Ga_{0.70}Sb$ superlattice.

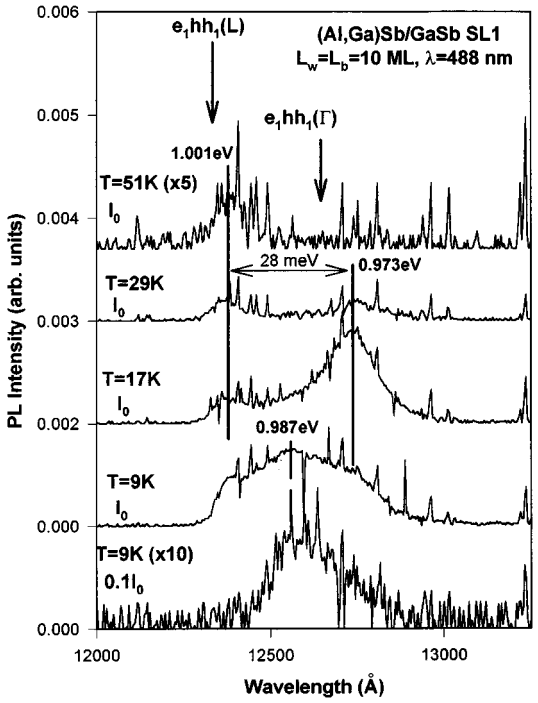

FIG. 8. Excitation intensity and temperature dependence of the luminescence spectra of sample SL1. Arrows show the calculated bottom of G and L minibands of a (10 ML)/(10 ML) $Al_{0.03}Ga_{0.97}Sb/Al_{0.27}Ga_{0.73}Sb$ superlattice.

The arrows in Figs. 7 and 8 correspond to Kronig-Penney calculations of the Γ and L minibands of the superlattice. Square potential profiles are assumed and the physical parameters used are the same as those used in Refs. 17 and 24. It is worth pointing that such calculations give a rather good account of the PL energies of Γ and L isolated $GaSb/Al_{0.3}Ga_{0.7}Sb$ quantum wells grown under similar conditions,[17,24] allowing one to use them in the superlattice case with some confidence. The widths of the first Γ and L minibands calculated assuming nominal SL period and composition are shown on Fig. 7. Their minima correspond rather well to the main peak and to the high-energy shoulder of sample SL2 (974 and 993 meV, respectively, to be compared with experimental values of 978 and 996 meV). Note that whereas in isolated 10-ML-wide $GaSb/Al_{0.3}Ga_{0.7}Sb$ quantum wells the ground state is of type L,[24,25] in the short-period superlattice, it is Γ type, due to the strong interwell coupling induced by the low Γ mass in (Al,Ga)Sb [$m_\Gamma(GaSb)=0.04m_0$]. We then tentatively assign the main PL peak in SL2 to $\Gamma-e_1hh_1$ transitions and the high-energy shoulder to weakly populated $L-e_1hh_1$ ones. In this sample, we assign the low-energy PL shoulder at 945 meV to impurity related transitions. Indeed, in similar (Al,Ga)/As/GaAs quantum heterostructures, growth interruptions are known to favor interface smoothening, but also somehow impurity incorporation.

Now, let us consider the blueshift of PL energies of sample SL1 relative to SL2. We model sample SL1 in terms of a square-well superlattice with some Al admixture. In Fig. 8, arrows show the calculated e_1/hh_1 energies of a (10 ML)/(10 ML) $Al_{0.03}Ga_{0.97}Sb/Al_{0.27}Ga_{0.73}Sb$ superlattice, which are in good agreement with experimental values. Theoretical Γ- and L-e_1hh_1 energies are 980 and 1005 meV, respectively, to be compared to 987 and 1001 meV for the main peak and high-energy shoulder in the PL spectra of SL1. This modeling is of course an oversimplification. However, it is in agreement with the detection of Al in (Al,Ga)Sb/GaSb quantum wells,[26] grown by MBE without growth interruptions. Using this interpretation, the low-energy shoulder in SL1, which is related to the high-energy shoulder (Fig. 8), could be assigned to a phonon replication. Indeed, L valleys remain indirect in the k direction in a (001)-grown superlattice and phonons are required for momentum conserving transitions (a situation similar to type-II X_{xy} GaAs/AlAs superlattices). The energy of LO_Γ phonons in GaSb is 28 meV and the optical phonon dispersion is very weak in this compound.[27]

IV. DISCUSSION

The mode of growth clearly influences the densities of states of III-V heterostructures. The samples SL2 and SL3 were obtained with interruption of the growth after each layer while no such interruption was made in the case of the sample SL1. For the samples SL2 and SL3, the interface roughness is small. For the sample SL1, numerous 1-ML-thick steps exist at the interfaces and the number of atoms in an interfacial position is larger than for SL2 and SL3. The role of interfaces is expected to be higher for SL1 than for SL2 and SL3.

The GaSb/bulk $Al_{0.3}Ga_{0.7}Sb$ interface (Fig. 5) has been obtained with growth interruption as SL2 and the interface roughness must be small. The spectral DOS of the interface is characterized by the broadening of the main peak at the top of the valence band. This broadening could be attributed to the presence of point defects such as vacancies and antisites at the interface. Indeed DOS calculations performed for III-V binary semiconductors expect that defects give states in this energy range.[28,29]

The pronounced peak observed for SL2 in the energy range II at ≈ -6 eV is absent in the other $Al_{0.3}Ga_{0.7}Sb$ systems (Figs. 3 and 5). Indeed, no marked structure is seen in the DOS of the bulk $Al_{0.3}Ga_{0.7}Sb$ and the $GaSb/Al_{0.3}Ga_{0.7}Sb$ interface, which are similar in this energy region. As a consequence, the peak II is not characteristic of physicochemical interactions between the wells and the barriers.

We have seen in Fig. 5 that the peak II is accompanied by a narrowing of the main peak of SL2 and a shift of this peak towards higher binding energies. A narrowing of the main peak is also observed simultaneously to the presence of a pronounced peak II in the case of the single quantum well between two barriers in the arsenide sample QW1 (Fig. 4). Then the presence of a pronounced peak II is accompanied by changes of the main peak and these changes (increase of binding energies and narrowing of the peak) can be explained by a partial localization of the states. We have underlined that in the bulk ternary compound, the Al $3p$ states are hybridized with the other states over the whole valence band. A partial localization of the Al $3p$ DOS, i.e., a loss of their extended character, is accompanied by a dehybridization of these states. This agrees with the disappearance of the structure due to Al $3p$–Sb $5s$ hybridized states in SL2.

The dehybridization is made easier when the mixing of

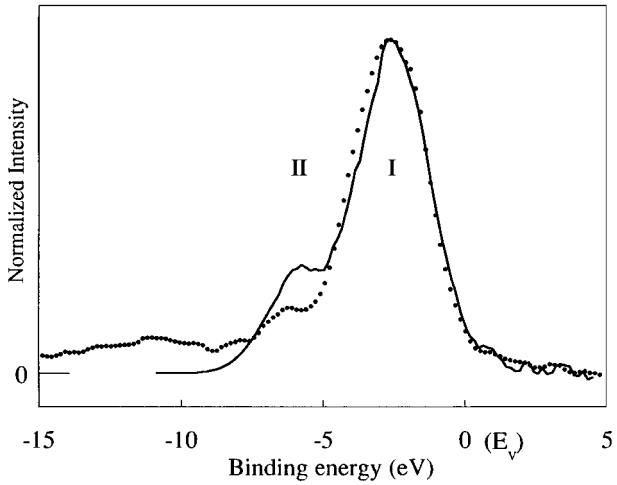

FIG. 9. Comparison of the Al 3p spectral DOS for the GaSb/$Al_{0.3}Ga_{0.7}$Sb superlattice SL2 (solid line) and for the GaSb/$Al_{0.3}Ga_{0.7}$As superlattice SL3 (dots).

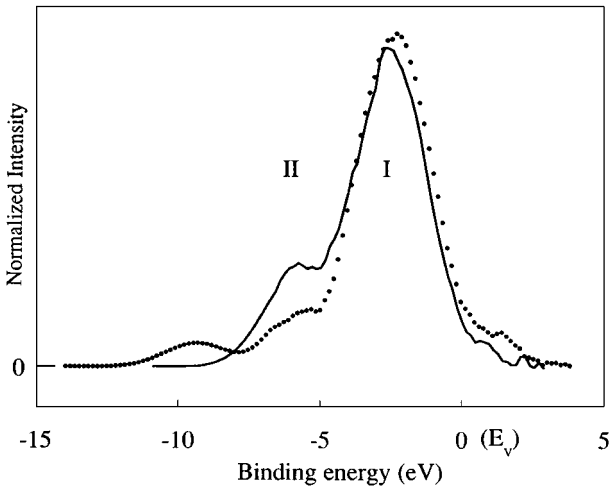

FIG. 10. Comparison of the AL 3p spectral DOS for bulk $Al_{0.3}Ga_{0.7}$Sb (dots) and for GaSb/$Al_{0.3}Ga_{0.7}$Sb superlattice SL2 (solid line). The curves are normalized with respect to the area.

states between neighboring atoms is smaller. Then, the binding between different atoms is weaker. This occurs if the difference between the cation and anion atomic numbers increases. Therefore one expects that the dehybridization is stronger in the antimonides than in the arsenides. The partial localization of the Al 3p states and their redistribution in energy is easier. This is in agreement with the fact that the changes of the Al 3p DOS are larger for antimonide superlattice SL2 than for arsenide superlattice SL3 (Fig. 9).

In the range of the peak II, the SL2 spectral DOS is higher than that of the bulk and the contrary is observed for SL3. One could expect that this increase of the spectral DOS is due to an increase of the Al 3p DOS and/or an increase of the transition probabilities from Al 3p states to the Al 1s hole.

The radiative recombination probability of a valence electron to a core hole varies with the more or less extended character of the valence states. The less extended are the valence states, the larger is the emission probability.[18] In the energy range II, the Al 3p states are hybridized with the Al 3s states in the bulk and have a partial extended character. A decrease of the extended character of the states and of their hybridization in this energy range leads to an increase of the 3p-1s emission probability. The emission probability also increases in the range of the main peak. Indeed a localization of the Al 3p states in this range is observed. Then, the emission probability increases in the entire energy range of the valence band and, as mentioned in Sec. II, it can be considered constant over the whole energy distribution of the Al 3p states.

Change observed in the energy range II for SL2 spectral DOS cannot be explained by an increase of the Al 3p-like character state number in the superlattice with respect to bulk $Al_{0.3}Ga_{0.7}$Sb. From the curves in Fig. 3, which are normalized with respect to the maximum intensity, the increase of this number should be very important. On the contrary, due to the high quality of the sample preparation, the concentration of different elements is the same in the bulk and the SL2 superlattice. We suggest the observed change is due to a redistribution of the Al 3p DOS. This is illustrated in Fig. 10 where the curves are normalized with respect to the area. From these curves, a redistribution of the Al 3p DOS towards higher binding energies and a narrowing of the peaks are clearly seen. These changes are in agreement with the partial localization of the Al 3p states suggested above.

Then the observation of the well resolved peak II suggests that a redistribution of the Al 3p states takes place in the heterostructures. This is characteristic of the two-dimensional (2D) character of the states in the studied heterostructures. The localization of the states that accompanies the change of the long-range order in the growth direction completely dominates the interface effects in the case of SL2 and SL3. As an example, the main peak is narrower in SL2 than in the bulk whereas the reverse is true at the interface. Moreover, the shape of the peak II is similar for both SL2 and SL3 (Fig. 9).

For SL1, the peak II and the narrowing of the main peak are not observed (Fig. 3). The spectral DOS is slightly larger than that of the bulk in the region II and spreads towards the ionic gap. The emission around -5 to -8 eV can be attributed to the presence of point defects in agreement with calculated DOS.[28,29] As mentioned above, from these theoretical predictions, one expects also a broadening of the main peak, at the top of the valence band. Indeed, the peak I of SL1 is wider than that of SL2 but similar to that of the bulk, thus narrower than that of the interface (Fig. 5). For SL1, states related to the presence of defects are partially observed and bidimensionality effects are weak. Competition exists between interface and bidimensionality effects. This is tentatively attributed to the fact that the interface roughness is larger than in SL2.

As mentioned in the photoluminescence analysis, the simplified model of the optical transitions in SL1 assumes some intermixing of Al between wells and barriers. Its origin is unknown: surface segregation of Ga or Al during growth, interdiffusion, or interface roughness (a pseudosmooth interface is somehow equivalent to an intermixed interface). It appears that some correlation exists with the EXES results.

Indeed, the SL1 valence band is more ''alloylike'' (or disordered) than that of SL2, as Fig. 3 shows. The presence of AlSb in the wells can explain that the bidimensionality effects can be more spreaded out in SL1 than in SL2.

In summary, as previously shown for other systems,[30] the Al $3p$ DOS has a large sensitivity to the atomic arrangement. Its analysis elucidates the character of the valence states in the III-V compounds, making the effect due to the bidimensionality identifiable in the range where the valence states are strongly hybridized. We have shown that the bidimensionality effect dominates when growth interruption allows very smooth interfaces to be present in superlattices.

Let us discuss now the faint structures present above E_v in the bulk and SL2 and not in SL1 (Fig. 6). These emissions can be identified as the radiative recombination of core excitonic states created simultaneously with the $1s$ core hole. Then these excitonic states must have a p character. The conduction-band minimum has mostly s-like character and the empty p states are located ≈ 1.4 eV above the bottom of the conduction band.[31] In the bulk, we identify the structure at 1560.3 eV (Table II) with an excitonic state located just below the bottom of the conduction band and having a p-hybridized s character. The structure at 1561.4 eV is identified as the recombination from an excitonic state located just below the states having predominant Al $3p$-like character. The distance between both the observed structures (1.1 eV) is consistent with the 1.4-eV energy difference between the empty states. The symmetry of the states justifies that the intensity of the high photon energy structure is the larger.

For the $GaAs/Al_{0.3}Ga_{0.7}As$ superlattice, we have previously shown that the Al core exciton binding energy in the barriers exceeds by 0.4 eV that in the bulk.[13] Similarly, the binding energy of the SL2 exciton exceeds that of the bulk by 0.8 eV. Moreover one expects that the structure is more intense in SL2 than in SL1 because the localization of states is larger in SL2. Indeed an excitonic structure is seen for SL2 and not for SL1. This confirms that stronger localization of DOS exists for small interface roughness.

ACKNOWLEDGMENT

This work has been partially supported by the EU through Contract No. ERBCHRXCT940464.

[1] J. R. Chelikowsky and M. L. Cohen, Phys. Rev. B **14**, 556 (1976).
[2] B. I. Min, S. Massidda, and A. J. Freeman, Phys. Rev. B **38**, 1970 (1988).
[3] E. T. Yu, E. T. Croke, D. H. Chow, D. A. Collins, M. C. Phillips, T. C. McGill, J. O. McCaldin, and R. H. Miles, J. Vac. Sci. Technol. B **8**, 908 (1990).
[4] Z. Q. Li and W. Pötz, J. Vac. Sci. Technol. B **9**, 2251 (1991).
[5] C. Sénémaud, A. Gheorghiu, and L. Ley, Phys. Rev. B **43**, 12 413 (1991).
[6] B. K. Agrawal, P. S. Yadav, S. Kumar, and S. Agrawal, Phys. Rev. B **52**, 4896 (1995).
[7] R. Ludeke, L. Ley, and K. Ploog, Solid State Commun. **28**, 57 (1978).
[8] R. L. Johnson, J. H. Fock, L. Ley, and M. Cardona, in *Proceeding of the 17th International Conference on the Physics of Semiconductors*, edited by J. D. Chadi and W. A. Harrison (Springer, New York, 1985), p. 1239.
[9] D. H. Ehlers, F. U. Hillebrecht, C. T. Lin, E. Schönherr, and L. Ley, Phys. Rev. B **40**, 3812 (1989).
[10] M. T. Sieger, T. Miller, and T.-C. Chiang, Phys. Rev. B **52**, 8256 (1995).
[11] F. Vergand, P. Jonnard, and C. Bonnelle, Europhys. Lett. **10**, 67 (1989).
[12] F. Vergand, P. Jonnard, C. Bonnelle, C. Deparis, and J. Massies, J. Phys. Condens. Matter **3**, 3433 (1991).
[13] F. Vergand, P. Jonnard, M. Kefi, C. Bonnelle, C. Deparis, and J. Massies, J. Phys. Condens. Matter **5**, 1691 (1993).
[14] H. Sakaki, M. Tanaka, and J. Yoshino, Jpn. J. Appl. Phys. **24**, L417 (1985).
[15] M. Gurioli, A. Vinattieri, M. Colocci, A. Bosacchi, and S. Franchi, Appl. Phys. Lett. **59**, 2150 (1991).
[16] N. Ikharashi, M. Tanaka, H. Sakaki, and K. Ishida, Appl. Phys. Lett. **60**, 1360 (1992).
[17] J. Massies, M. Leroux, P. Vennegues, S. Laügt, and Y. Martinez, J. Cryst. Growth **160**, 211 (1996).
[18] C. Bonnelle, *Annual Report C 1987* (Royal Society of Chemistry, London, 1987), pp. 201–272.
[19] C. Bonnelle and F. Vergand, J. Chim. Phys. **86**, 1293 (1989).
[20] C. Bonnelle, F. Vergand, P. Jonnard, J.-M. André, P.-F. Staub, P. Avila, P. Chargelègue, M.-F. Fontaine, D. Laporte, P. Paquier, A. Ringuenet, and B. Rodriguez, Rev. Sci. Instrum. **65**, 3466 (1994).
[21] (a) P.-F. Staub, J. Phys. D **27**, 1533 (1994); (b) **28**, 252 (1995); (c) X-ray Spectrum (to be published).
[22] P.-F. Staub, P. Jonnard, F. Vergand, J. Thirion, and C. Bonnelle, X-ray Spectrom. (to be published).
[23] A. Mujica and A. Muñoz, Solid State Commun. **81**, 961 (1992).
[24] M. Leroux and J. Massies, Appl. Phys. Lett. **68**, 54 (1996).
[25] P. V. Giugno, A. Convertini, R. Rinaldi, R. Cingolani, J. Massies, and M. Leroux, Phys. Rev. B **52**, R11591 (1995).
[26] C. Gerardi, A. Capello, and R. Cingolani (unpublished).
[27] O. Madelung, *Semiconductors: Physics of Group IV Elements and III-V Compounds*, edited by K.-H. Hellwege and O. Madelung, Landolt-Börnstein, New Series, Group III, Vol. 17, Pt. a (Springer-Verlag, Berlin, 1991), p. 114.
[28] P. J. Lin-Chung and T. L. Reinecke, Phys. Rev. B **27**, 1101 (1983).
[29] M. J. Puska, J. Phys. Condens. Matter **1**, 7347 (1989).
[30] M. Kefi, P. Jonnard, F. Vergand, C. Bonnelle, and E. Gillet, J. Phys. Condens. Matter **5**, 8629 (1993).
[31] R. Magri, S. Froyen, and A. Zunger, Phys. Rev. B **44**, 7947 (1991).